HHS Public Access

Author manuscript

Annu Int Conf IEEE Eng Med Biol Soc. Author manuscript; available in PMC 2021 September 14.

Published in final edited form as:

Annu Int Conf IEEE Eng Med Biol Soc. 2018 July ; 2018: 4752–4755. doi:10.1109/EMBC.2018.8513208.

Simulations of a birdcage coil B_1^+ field on a human body model for designing a 3T multichannel TMS/MRI head coil array

Lucia I. Navarro de Lara,
Athinoula A. Martinos Center for Biomedical Imaging, Massachusetts General Hospital, Charlestown, MA 02129 USA

Laleh Golestani Rad,
Athinoula A. Martinos Center for Biomedical Imaging, Massachusetts General Hospital, Charlestown, MA 02129 USA.

Sergey N. Makarov [Member, IEEE],
Department of Electrical and Computer Engineering at the Worcester Polytechnic Institute, Worcester, MA 01609, USA. He is also with the Athinoula A. Martinos Center for Biomedical Imaging at the Massachusetts General Hospital, Charlestown, MA 02129, USA

Jason Stockmann,
Athinoula A. Martinos Center for Biomedical Imaging, Massachusetts General Hospital, Charlestown, MA 02129 USA.

Lawrence L. Wald,
Athinoula A. Martinos Center for Biomedical Imaging, Massachusetts General Hospital, Charlestown, MA 02129 USA.

Aapo Nummenmaa
Athinoula A. Martinos Center for Biomedical Imaging at the Massachusetts General Hospital, Charlestown, MA 02129, USA

Abstract

This article considers a new type of integrated multichannel Transcranial Magnetic Stimulator and Magnetic Resonance Imaging (TMS/MRI) system at 3T that is currently being designed. The system will enable unprecedented spatiotemporal control of the TMS-induced electric fields (E-fields) with simultaneous rapid whole-head MRI acquisition to record the brain activity. A critical design question is how TMS coil elements interact with the transmit field (B_1^+) of the volume coil integrated in 3T MRI systems. In general, the TMS coils are not designed to have any resonant characteristics at the MRI frequency, they may potentially disturb the RF field due to the eddy currents induced. This is especially a concern with a multichannel TMS setup where the subject's head will be largely covered with the stimulation coils. Therefore, we investigated this problem by computational simulations with realistic TMS coil geometries and a birdcage transmit coil in conjunction with a human body model. We compared the B_1^+ interaction effects of a commercially available MR-compatible TMS coil with our coil prototype. In both cases, the results show small local changes in the transmit field $B_1^+$of the birdcage coil. Maximal Average

(lnavarrodelara@mgh.harvard.edu).

Specific Absorption Rate (SAR) values over 1g tissue were found to be slightly lower when the TMS elements were present. We conclude that it should be feasible and safe to use the conventional body transmit coil even when an array of TMS coils is used.

I. INTRODUCTION

Combining neuroimaging modalities with non-invasive brain stimulation techniques has contributed significantly to our understanding of brain anatomy, physiology and pathology. The integration of transcranial magnetic stimulation (TMS) with functional magnetic resonance imaging (fMRI) was presented for the first time by Bohning et al. in 1999 [1]. The TMS-fMRI combination appears especially promising for providing quantitative measures of the stimulation as it enables localizing the TMS-induced activations with millimeter-scale resolution. Additionally, this approach could help answer unresolved questions concerning causality in fMRI activation studies as well as to understand the network-level brain connectivity measures and how these may be modulated by TMS.

A critical barrier of the concurrent TMS-fMRI studies has been that the contemporary helmet-shaped multichannel RF receive coil arrays cannot be employed due to the fact that the TMS coils need to be placed on top of the subject's scalp. The inability to use the surface coil arrays results in loss of sensitivity for MR signal detection [2] and inability to employ parallel imaging techniques [3,4]. New methods and RF-coil instrumentation approaches have been introduced to mitigate this issue [5] as well as to solve other related technical challenges [6–8]. Another fundamental limitation for TMS-fMRI studies is that once the coil is positioned and the subject is moved inside the scanner bore, the position of the stimulation coil cannot be changed. If the subject moves and the TMS coil is displaced, the stimulation may become less efficient and/or targeted to an undesired location. To address this key limitation as well as to enable even broader range of potential applications, a multichannel TMS/MRI head coil array for 3 T is currently under development (see Fig.1).

Multichannel TMS [9] is an emerging technology that allows multiple sites to be stimulated simultaneously or sequentially under electronic control. The obvious benefit of the electronic targeting is that no physical movement of the coils is necessary to correct or modify the target location to be stimulated, thus providing an effective solution especially for TMS/fMRI experiments. This novel technique combined with simultaneous rapid whole-head MRI acquisition will also enable to monitor brain activity on-line enabling closed loop applications, opening up new avenues for basic neuroscience research and developing individualized quantitative therapeutic applications. This type of integrated multichannel TMS/MRI array is currently under development through funding support from the NIH BRAIN Initiative.

Building the new integrated stimulation/imaging system presents several engineering challenges. At the outset, the MR compatibility of the materials used in the fabrication of the TMS coils must be determined. This can be done by acquiring MR images with the materials placed into the vicinity of a phantom and quantifying possible susceptibility effects and artefacts. Another key issue in the development of the TMS/MRI coil array is the assessment of the influence of the conducting elements (TMS coils) on the RF excitation

from the MR scanner. The critical question is if a standard body coil can be used for transmission when several TMS coils are positioned next to the subject's head. This issue has not been previously systematically investigated and therefore we studied the effects of the planned multichannel TMS system on the transmit field (B_1^+) of a birdcage coil based on electromagnetic (EM) simulations.

II. METHODS

The overarching goal of the TMS/MRI project is to construct an MRI compatible 16×3=48 multichannel TMS system and integrate that with a 32 channel RF whole head coil array. The basic TMS element of the multichannel stimulation coil consists of 3 orthogonal coils (X, Y and Z) that can be independently activated. This system will allow multi-target stimulation (simultaneously or sequentially) while concurrently recording functional brain activity from the entire brain. Fig. 1A shows a schematic layout of the planned 3 Tesla multichannel TMS/MRI whole-head coil. A photograph of a TMS element prototype built by Tristan Technologies (San Diego, USA) is shown in Fig.1B. An illustration of the integrated multichannel TMS/MRI array coil concept in the MR scanner is shown in Fig.1C

A 3T high pass birdcage coil was modeled in HFFS (Ansys, USA). It was tuned and matched with an ASTM gel whole body phantom as load. Three models were built: (i) the birdcage coil loaded only with the phantom, (ii) the coil loaded with a commercial MR compatible TMS coil over the left hemisphere of the phantom, and (iii) the coil loaded with the phantom and 16 three-axis TMS elements distributed over the phantoms head (see Fig.2A-C). The commercial MR compatible TMS coil (MagVenture MRi-B91) was included in the simulations to compare the effects of this standard coil used in concurrent TMS/fMRI experiments with our new three-axis coil design for the multichannel TMS system. For the EM simulations, the birdcage coil was modeled with all lumped elements being defined as 50 Ω ports [10]. Once the EM simulation was done, RF co-circuit simulations were run using the calculated S parameters to find the optimal capacitor values for tuning and matching the coil. These values were only optimized for the "no TMS coil" case. The same values were subsequently used for the simulations with the different TMS coil configurations present. All simulations were run on a Linux Server. Calculated B_1^+ fields over the central sagittal and coronal planes in the phantom were visualized in HFFS.

For the purpose of quantification of the effects, the average B_1^+ fields were calculated in surfaces parallel to the skull at different depths: at 1cm, 2cm and 3cm (see Fig.3). To evaluate the homogeneity of the transmit field, standard deviation of the field data over the three surfaces defined above were calculated. Field homogeneity is critical to ensure neither artifacts nor intensity changes will be present in acquired images. Finally, average SAR values over 1g tissue were calculated for the 3 surfaces described above for the three simulation setups.

III. RESULTS

The simulated B_1^+ fields for each case are shown in Fig 4. over the coronal central plane and in Fig.5 for the central sagittal plane. In both cases, fields either slightly increase or decrease

in different regions. Arrows in the subfigures point to these local changes. The average B_1^+ field over the 3 different surfaces for the three simulations are summarized in Table I. For the commercial MR compatible TMS coil, the average field increase at 1 cm was 2.6% compared to the no coil case. At 2 cm the average field decreases 0.25% and at 3 cm, it is 2.1 % less. In the case of the 3-axis TMS coil array, the average field is always lower than in the “no coil” case. At 1 cm the average is lower only by 3.7%, at 2 cm by 4.2% and at 3 cm by 7.2%.

The standard deviation of the B_1^+ field over the 3 different surfaces for the three simulated configurations are summarized in Table II. For the commercial MR compatible TMS coil, the standard deviation of the field is at 1 cm 4.2% higher than the no coil case. At 2 cm, it is 6.3% higher than the case with no coil present. At the typical target depth of the TMS, at 3 cm this trend changes; the standard deviation is 3.1 % lower than the case with no coil. In the case of the 3-axis TMS coil array, the standard deviation of the field over the three surfaces is always lower than the no TMS coil case. At 1 cm, it is 1% lower, at 2 cm 4% lower and at 3 cm, 2.6% lower.

The maximal calculated average SAR values over 1g tissue are listed in Table III. Highest B_1^+ values were found on the neck (see Fig.5), and average SAR maxima over the defined surfaces (see Fig.3) were all found close to that region. For the commercial TMS coil, the maximum average SAR increased 18% compared to the no coil case evaluated at 1 cm depth surface. Over the 2 cm depth surface, the maximum average SAR only was 7 % higher, and at 3 cm depth, the maximum average SAR was 11% lower than the average SAR value of the no coil case. For the multichannel TMS setup, the average SAR values were in all cases lower than the no TMS coil reference case.

IV. DISCUSSION

How TMS coils change the RF transmission field in the MRI scanners has not been generally investigated yet, which was a key motivation for our study. Despite the obvious importance of this topic from safety perspective, we did not find any detailed simulation studies considering the interactions between the TMS and RF coil(s). Our primary goal here was to carry out simulations to assess the homogeneity of transmission field of a 3 T birdcage coil when inserting a multichannel TMS coil array into the bore.

Another important issue was to quantify the possible increase of the SAR values due to the presence of the TMS coils. For comparison, we carried out identical simulations for a commercially available MR compatible TMS coil (MagVenture MRi-B91), which is currently being used in concurrent TMS/fMRI experiments. We used realistic models for the RF coil, TMS coil(s), as well as the human head. The results of our study can be utilized for guiding the design of the integrated TMS/MRI coil system, but the presented simulation framework can be more generally adopted for similar problems in integrating TMS with MRI as well.

Our simulations show minimal local changes in the field both in the case of the conventional TMS coil and multichannel TMS coil array. Perhaps surprisingly, the multichannel TMS

array configuration did not result in substantially more distortions of the B_1^+ field than the commercially available figure-of-eight coil. The SAR calculation also indicate lower values for the multichannel TMS array than for the commercial TMS coil. An important point to notice is that for the commercial MR compatible TMS coil, these changes may depend on the position and orientation of the coil used for a particular study or subject (*e.g.,* stimulation of motor cortex *vs.* frontal cortex). For the multichannel TMS case, the coil elements will be in highly similar positions inside the MRI scanner bore (the coil position will be adjustable radially), which means that transmit field will remain relative constant across studies/subjects. However, in designing and fabricating the TMS coils it is important to avoid any resonances that might occur near the RF transmit frequency. The cases in which such resonances occur would be an interesting topic for further investigation.

V. CONCLUSION

Our computational analysis of the interactions between the TMS coils and RF birdcage transmit coils shows small enhancements and attenuations of the B_1^+ fields. However, the overall homogeneity of the birdcage coil transmit field is only marginally affected. The average SAR values over 1 g tissue are lower than the values obtained in the no TMS coils case. Therefore, our results suggest that placing a multichannel TMS coil array into the MR environment poses no significant issues for the RF transmission either from technical or safety standpoints.

ACKNOWLEDGMENT

We want to thank H. Corfitzen (MagVenture, Farum, Denmark) providing information about the dimensions of the MagVenture MR compatible TMS coil. We also thank Dr. Yoshio Okada from Moment Technologies and Dr. Bastien Guerin and Dr. Thomas Witzel from MGH Martinos Center for valuable discussions on the subject.

**Research supported by NIH R00EB015445, R01MH111829 and NIH K99EB021349.

REFERENCES

[1]. Bohning DEet al. “Echoplanar BOLD fMRI of brain activation induced by concurrent transcranial magnetic stimulation.” in Investigative Radiology, 33(6):336–340,1998 [PubMed: 9647445]

[2]. Keil Bet al..“A 64-channel 3T array coil for accelerated brain MRI.” in Magnetic Resonance in Medicine, 70(1):248–58, 2013. [PubMed: 22851312]

[3]. Pruesmann KPet al. “SENSE: Advances in sensitivity encoding with arbitrary k-space trajectories.” In Magnetic Resonance Imaging, 46(4): 638–651, 2001.

[4]. Griswold MAet al.“Generalized autocalibrating partially parallel acquisitions (GRAPPA).” in Magnetic Resonance Imaging, 47: 1202–1210, 2002.

[5]. Navarro de Lara Let al. “A novel coil array for combined TMS/fMRI experiments at 3T” in Magnetic Resonance in Medicine, 74(5):14921501, 2015.

[6]. Weiskopf Net al.“Image artifacts in concurrent transcranial magnetic stimulation (TMS) and fMRI caused by leakage currents: modeling and compensation.” in Journal of Magnetic Resonance Imaging, 29(5):1211–7, 2009 [PubMed: 19388099]

[7]. Bestmann Set al. “On the synchronization of transcranial magnetic stimulation and functional echo-planar imaging”, in Journal of Magnetic Resonance Imaging, 17(3):309–16, 2003 [PubMed: 12594720]

[8]. Moisa Met al.“New coil positioning method for interleaved transcranial magnetic stimulation(TMS)/ functional MRI (fMRI) and its validation in a motor cortex study”, in Journal of Magnetic Resonance Imaging, 29(1):189–97, 2009. [PubMed: 19097080]

[9]. Ruohonen J and Ilmoniemi R. “Focusing and targeting of magnetic brain stimulation using multiple coils” in Medical and Biological Engineering and Computing, 36:297–301,1998 [PubMed: 9747568]

[10]. Kozlov M and Turner R “Fast MRI coil analysis based on 3-D electromagnetic and RF circuit co-simulation.” in Journal of Magnetic Resonance Imaging, 200(1):147–52,2009

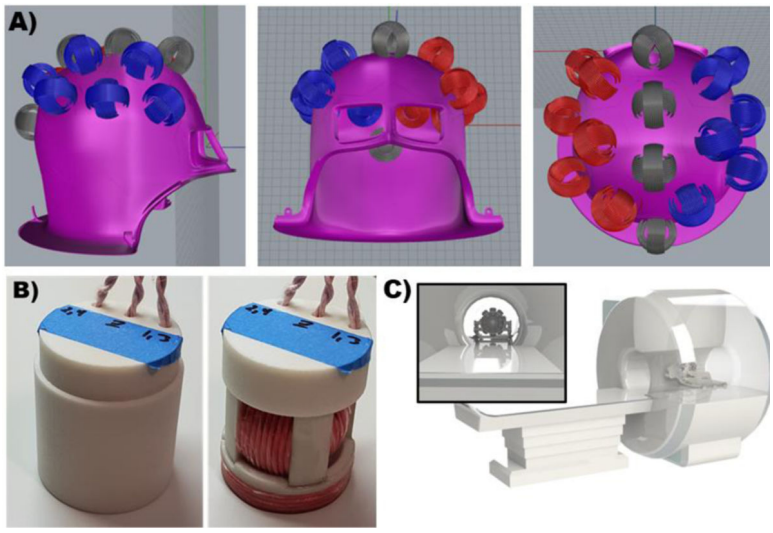

Figure 1. A)
Different views of the first multichannel TMS/MRI whole head coil array prototype. **B)** Photographs of the 3-axis TMS prototype. **C)** Multichannel TMS/MRI whole head coil array concept visualized in the MR scanner. (Illustration C courtesy of Anthony Mascarenas, Tristan Technologies)

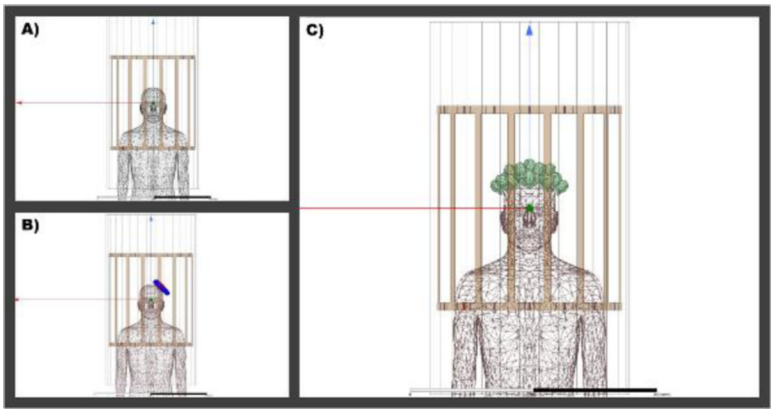

Figure 2.

Schematic of the simulation setup. **A)** RF coil loaded only with the phantom. **B)** RF coil loaded with the phantom and the commercial MR compatible TMS coil. **C)** RF coil loaded with the phantom and the 4×4 3-axis TMS coil array.

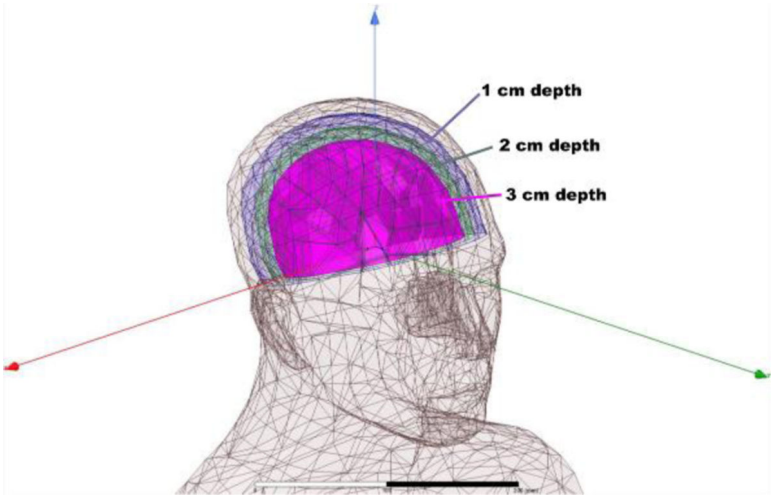

Figure 3.
Surface definition for B1+ field quantification. Three surfaces were created at 1cm, 2cm and 3cm distance from the skull.

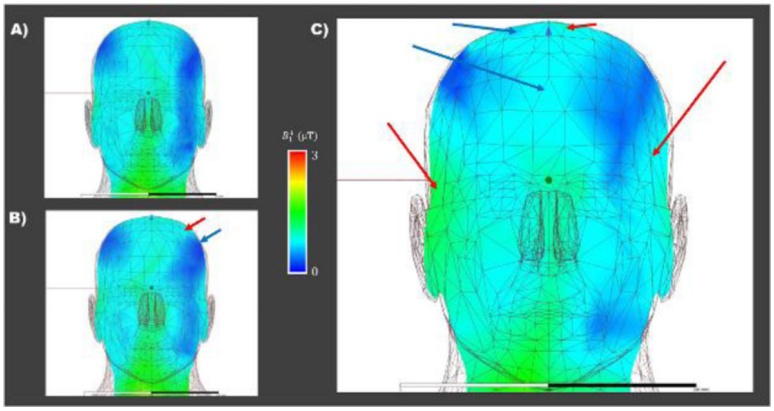

Figure 4.

B_1^+ results over the central coronal plane. **A)** Birdcage coil loaded only with the phantom **B)** Birdcage coil loaded with the phantom and the commercial MR compatible TMS coil. **C)** Birdcage coil loaded with the phantom and the 4×4 3-axis TMS coil array. Arrows show either areas with increased field (red arrows) or decreased field (blue) compared to the no coil case shown in A. The TMS coil placement for all cases is as shown in Fig 2, respectively.

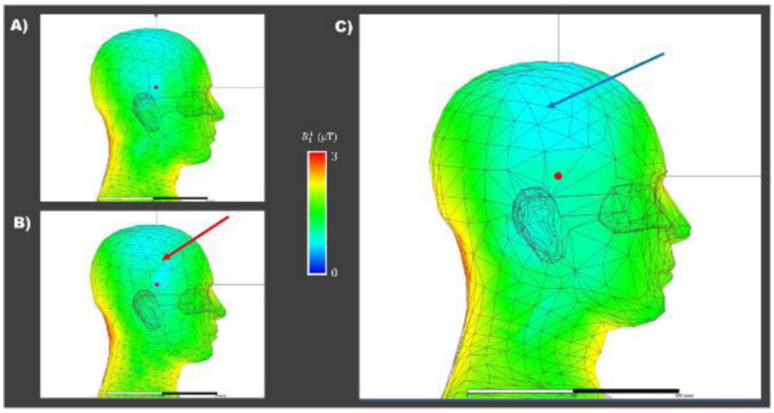

Figure 5.

B_1^+ results over the central sagittal plane. A) Birdcage coil loaded only with the phantom B) Birdcage coil loaded with the phantom and the commercial MR compatible TMS coil placed as shown in Fig 2.B, and C) Birdcage coil loaded with the phantom and the 4×4 3-axis TMS coil array. Arrows show either areas with increased field (red arrow) or decreased field (blue arrow) compared to the no coil case shown in A.

TABLE I.

SIMULATED AVERAGE B_1^+ FIELD OVER THE SURFACE AT 1CM, 2CM AND 3CM DEPTH

Depth	Average B_1^+ (μT)		
	No Coil	*Commercial TMS coil*	*3-axis TMS coil array*
1 cm	1.044	1.071	1.005
2 cm	0.998	0.995	0.956
3 cm	0.936	0.917	0.868

TABLE II.

STANDARD DEVIATION OF THE B_1^+ FIELD OVER THE SURFACE AT 1CM, 2CM AND 3CM DEPTH

Depth	Standard deviation B_1^+ (μT)		
	No coil	*Commercial TMS coil*	*3-axis TMS coil array*
1cm	0.449	0.468	0.445
2 cm	0.418	0.441	0.401
3 cm	0.381	0.380	0.371

TABLE III.

MAXIMAL AVERAGE SAR OVER 1G TISSUE OVER THE SURFACE AT 1CM, 2CM AND 3CM DEPTH

Depth	**Maximal Average SAR over 1g (W/Kg)**		
	No coil	***Commercial TMS coil***	***3-axis TMS coil array***
1 cm	10.745	12.726	10.406
2 cm	9.606	10.285	9.085
3 cm	8.214	7.304	7.903